Antibacterial Efficacy of Zinc and Zirconium Based Metal Organic Frameworks against Escherichia coli and Staphylococcus aureus

by Perpustakaan IIK Bhakti Wiyata

Submission date: 04-May-2026 01:46PM (UTC+0700)
Submission ID: 2392274386
File name: 4._bioconf_icolist2024_01025_-_Iqbal_Aljabir_Pujiono.pdf (925.95K)
Word count: 4205
Character count: 22619

Antibacterial Efficacy of Zinc and Zirconium Based Metal Organic Frameworks against *Escherichia coli* and *Staphylococcus aureus*

Tri Ana Mulyati[1*], *Juni* Ekowati[2], *Yohanes Andy* Rias[3], *Binti* Mu'arofah[4], *Siska Kusuma* Wardani[4], and *Fery Eko* Pujiono[1]

[1]Departement of Pharmacy, Institut Ilmu Kesehatan Bhakti Wiyata, Kediri, Indonesia
[2]Departement of Pharmaceutical, Airlangga University, Surabaya, Indonesia
[3]Departement of Nursing, Institut Ilmu Kesehatan Bhakti Wiyata, Kediri, Indonesia
[4]Departement of Medical Laboratory Technology, Institut Ilmu Kesehatan Bhakti Wiyata, Kediri, Indonesia

Abstract. Bacterial resistance to antibiotics, affecting both Gram-positive and Gram-negative bacteria, remains a major challenge. Zn-MOF and Zr-MOF offer promising antibacterial properties through metal ion release and membrane disruption. In this research, Zn-MOF and Zr-MOF were synthesized using the solvothermal method and antibacterial tests were carried out. The solids formed were then characterized using ATR-FTIR, XRD and SEM. The results of analysis using ATR-FTIR show that the Zn-MOF functional groups appear at wavelengths 3666-3036 cm^{-1}(νO-H), 1587 cm^{-1} (ν–OCO-sym), 1392 cm^{-1} (ν–OCO-asym), 837 cm^{-1} (νC-H), 748cm^{-1} (νC=C) and 651cm^{-1}(νZn-O) while the Zr-MOF functional group appears at a wavelength of 3658-3174 cm^{-1} (νO-H), 1562cm^{-1} (ν–OCO-sym), 1390cm^{-1} (ν–OCO-asym), 823cm^{-1} (νC-H), 742cm^{-1} (νC=C) and 563cm^{-1} (νZr-O). The results of XRD analysis show that the characteristic peak of Zn-MOF is at 2θ 6.8°; 9.6°; 13.72°; 15.44°; 20.6° while the distinctive peak of Zr-MOF is shown at 2θ 7.32°; 8.48°; 11.9°; 14.0°; 14.6°; and 17.0°. Meanwhile, SEM results show that Zn-MOF has a cubic surface structure while Zr-MOF has aggregated particles with an irregular round shape. The results of the antibacterial test for *Staphylococcus aureus* showed that Zn-MOF (38.9 ± 1 mm) had a largest zone of inhibition, equivalent to the results of the antibacterial test for *Escherichia coli* showing that Zn-MOF (36.2±1 mm) has a largest zone of inhibition.

1 Introduction

Bacteria are tiny, single-celled prokaryotic microorganisms that commonly cause infectious diseases. One current issue is bacterial resistance. Bacterial resistance refers to the ability of bacteria to survive and reproduce even when exposed to antibiotics or antimicrobials that should inhibit their growth [1]. One cause of bacterial resistance is the formation of biofilms on bacterial surfaces, which increases their resilience to environmental changes

* Corresponding author: nanapujiono@gmail.com

antibiotic use [2–3]. Some common bacteria that cause infectious diseases include *Escherichia coli* (Gram-negative) and *Staphylococcus aureus* (Gram-positive).

Escherichia coli is a Gram-negative pathogenic bacterium that is rod-shaped and most found as the cause of infectious diseases. *E. coli* produces toxins that can damage host cells [4]. *Staphylococcus aureus* is a Gram-positive pathogenic bacterium. *Staphylococcus aureus* is spherical (cocci) in shape and is usually found in clusters resembling grapes. *Staphylococcus aureus* can produce various toxins, such as exfoliative toxins, enterotoxins, and toxic shock syndrome, which can damage host tissue and contribute to severe clinical symptoms [5–6]. *Escherichia coli* and *Staphylococcus aureus* develop antibiotic resistance through various mechanisms. *Escherichia coli* produces *β-lactamase* enzymes that degrade *β-lactam* antibiotics, rendering them ineffective [7], while *Staphylococcus aureus* can modify proteins, thereby reducing antibiotic affinity [8]. The mechanisms enable both bacteria to decrease intracellular antibiotic concentrations. Genetic mutations and horizontal gene transfer further disseminate resistance traits. Misuse and excessive use of antibiotics can accelerate resistance, making infections increasingly difficult to treat [9]. This underscores the importance of developing materials that can address the issue of bacterial resistance. One such material being developed as an antibacterial agent is a Metal-Organic Framework (MOF).

The development of MOFs as antibacterial materials cannot be separated from bacterial resistance. Metal-Organic Frameworks, or MOFs, are porous materials composed of metal ions or metal clusters connected by various organic ligands to form a framework [10]. The advantages of MOFs lie in their ability to be synthesized using different metal ions and ligands, allowing for the formation of MOFs with varying characteristics. MOFs exhibit high porosity and stability. Additionally, they can oxidize and depolarize the outer bacterial cell membrane, inhibiting bacterial protein synthesis. The central metal in MOFs can also damage bacterial proteins, decreasing bacterial activity [11].

Several studies have successfully developed metal–organic frameworks (MOFs) as antibacterial agents. Among them, MOF-74 and MOF-5—both of which are based on zinc ions—have demonstrated significant antibacterial activity. For instance, AbouAitah *et al.* [12] reported that Zn-based MOF-74 and MOF-5 were able to inhibit the growth of *E. coli* and *K. pneumoniae* by 80% to 99.9%. Similarly, Gao[13] found that UiO-66 (Zr-based MOFs) showed inhibitory effects against up to 90% of multidrug-resistant bacteria. These findings highlight the antibacterial potential of MOFs with different metal centers, particularly Zn and Zr. However, further studies are needed to explore and optimize Zn- and Zr-based MOFs with different synthesis approaches and ligands. Based on this background, this research focuses on the synthesis of Zn- and Zr-based MOFs and evaluates their antibacterial efficacy against *Escherichia coli* (Gram-negative) and *Staphylococcus aureus* (Gram-positive).

2 Experimental Details

2.1 Materials

Zinc (II) nitrate hexahydrate ($Zn(NO_3)_2 6H_2O$) (SigmaAldrich, 99 %), Zirconium tetracloride ($ZrCl_4$) (SigmaAldrich, 99.0%) 1,4-benzenedicarboxylic acid (H_2BDC) (SigmaAldrich, 99%), N'N-dimethylformamide (DMF) (Merck, 99.8 %), chloroform ($CHCl_3$) (Merck, 99.8 %), Mueller-Hinton Agar (MHA) (Merck, 99%).

2.2 The synthesis of Zn-MOF and Zr-MOF

At this stage, the synthesis of MOF is carried out using two different central metals, Zn and Zr, and the same ligand, 1,4-Benzenedicarboxylic acid (H_2BDC). The method used in this stage is solvothermal. The Zn-MOF synthesis procedure is a modification of Hu *et al.* [14], where 1.08 grams of $Zn(NO_3)_2.6H_2O$ and 0.198 grams of H_2BDC are dissolved in 30 mL of Dimethylformamide (DMF). The resulting solution is then placed in a 50 mL sealed vial and stirred for 30 minutes, followed by heating at 120°C for 24 hours in a static condition. The resulting mixture is cooled and decanted. Next, the obtained solid is washed with 30 mL of DMF for 24 hours, followed by two washes with 30 mL of chloroform every 24 hours. The resulting solid is then decanted and dried under vacuum at 60°C for 24 hours until it becomes dry. The resulting solid is then referred to as Zn-MOF.

The Zr-MOF synthesis procedure is a modification of Zulfa *et al.* [15], which involves dissolving 0.53 grams of Zirconium tetrachloride ($ZrCl_4$) and 0.34 grams of H_2BDC in 30 mL of dimethylformamide (DMF). The solution is then stirred for 30 minutes and heated in an oven at 120°C for 24 hours. The resulting product is cooled to room temperature overnight. The solution is then filtered, and the solid is washed with 30 mL of DMF and left overnight. The solid is further washed twice with 30 mL of chloroform. The washed solid is then dried at 50°C for 24 hours, forming Zr-MOF.

2.3 Characterization of Zn-MOF and Zr-MOF

All formed solids were characterized using X-ray diffraction (XRD), Attenuated Total Reflectance Fourier Transform Infrared Spectroscopy (ATR FTIR), and Scanning Electron Microscopy (SEM). XRD analysis was performed using a JEOL diffractometer with Cu Ka radiation (λ = 1.54056 Å) at 40 kV and 30 mA. Solid crystallinity measurements were conducted in the 5–50° range. Solid functional group analysis was carried out using Shimadzu's ATR-FTIR in the 400–4000 cm^{-1} wavenumber range. Surface analysis of the solids was performed using SEM (Zeiss EVO MA10).

2.4 The antibacterial activity evaluation

The antimicrobial properties of Zn-MOF and Zr-MOF against *Escherichia coli (Gram-negative) and Staphylococcus aureus (Gram-positive)* were conducted using the zone of inhibition measurement (ASTM E2149-13a) with a modified disc diffusion method from Elmehrath *et al.* [16]. Initially, 6 mm filter paper discs were saturated with Zn-MOF and Zr-MOF solutions at 2 mg/mL for 2 hours. Aseptically, 30 ml of sterile MHA (Mueller-Hinton agar) was solidified into a large petri dish (15 cm diameter). After the agar medium solidified, a sterile cotton swab was dipped into the bacterial suspension of *Escherichia coli* and *Staphylococcus aureus* and then evenly swabbed onto the surface of the MHA medium. The saturated filter paper discs (6 mm size) and amoxicillin antibiotic discs (as a control) were placed on the swabbed agar medium. The results were incubated for 18-24 hours at 37°C in an incubator, and the zone of inhibition formed was measured using calipers.

3 Results and Discussion

3.1 The synthesis of Zn-MOF and Zr-MOF

The synthesized Zn-MOF and Zr-MOF were synthesized by reacting the respective Zn and Zr metals with the ligand H_2BDC. The solvent used was DMF, and the method employed

was solvothermal. The formation of white solids after the reaction indicates the successful synthesis of Zn-MOF and Zr-MOF. Figure 1 illustrates the formation of Zn-MOF and Zr-MOF.

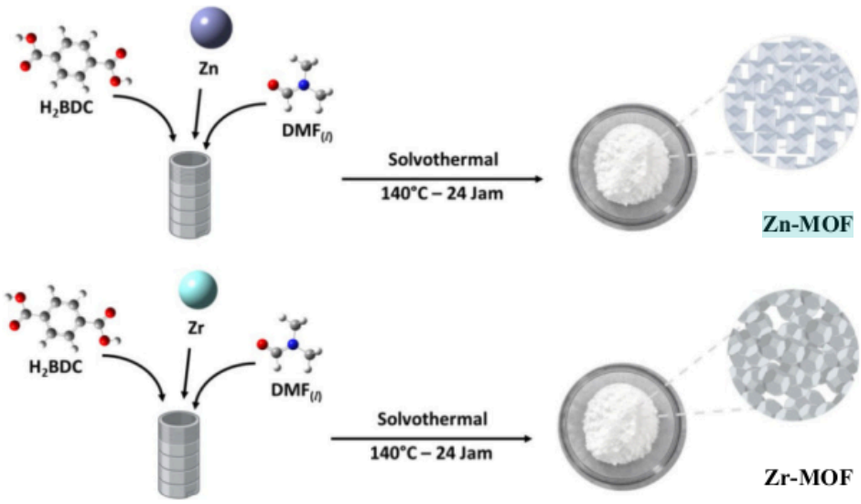

Fig 1. Illustration of Zn-MOF and Zr-MOF Formation via Solvothermal Method

3.2 Characterization of Zn-MOF and Zr-MOF

3.2.1 FTIR Analysis

The FTIR spectra of Zn-MOF and Zr-MOF are shown in Figure 2, while the analysis of characteristic functional groups of Zn-MOF and Zr-MOF is presented in Table 1. Based on Figure 2a and Table 1, it is found that several characteristic functional groups of Zn-MOF are present, including peaks at 3666 cm^{-1} (indicating O-H vibration due to the presence of water vapor, consistent with the research by Dahlan *et al.* [17] and Hu *et al.* [14] and broad peaks in the region of 3036 cm^{-1}. The subsequent peaks appear at wavenumbers 1587 cm^{-1} and 1392 cm^{-1}, corresponding to symmetric and asymmetric vibrations of carboxylate groups (-OCO-). These results align with the findings of Hu *et al.* [14] indicating the presence of C=O bonds in the ligands coordinated with Zn. The vibrations of C-H and C=C at wavenumbers 823 cm^{-1} and 742 cm^{-1}, respectively, are consistent with the research by Rocha [18]. The peak at 651 cm^{-1} in the fingerprint region indicates Zn-O vibrations. Hu *et al.* [14] also reported that the presence of Zn-O vibrations in the range of 500-600 cm^{-1} indicates the formation of Zn_4O metal clusters. This result further strengthens the successful formation of Zn-MOF.

The characteristic functional groups of Zr-MOF (Figure 2b) appear at wavenumbers 3658-3174 cm^{-1}, indicating O-H vibrations. This is consistent with the study by Tian *et al.* [19], which also reported O-H vibrations at a wavenumber of 3343 cm^{-1} due to surface water on Zr-MOF. In the FTIR spectrum of Zr-MOF, symmetric and asymmetric –OCO- vibrations were also found at wavenumbers 1562 cm^{-1} and 1390 cm^{-1}. These results align with the research by Nasrabadi *et al.* [20] and Tian *et al.* [19], who reported the presence of carboxylate ligand connections with Zr^{4+} in the FTIR spectrum. The peak at wavenumber 563 cm^{-1} indicates Zr-O vibrations, suggesting the formation of Zr_6O_4 clusters, as observed in the studies by Lin *et al.* [21]. These findings further support the successful formation of Zr-MOF.

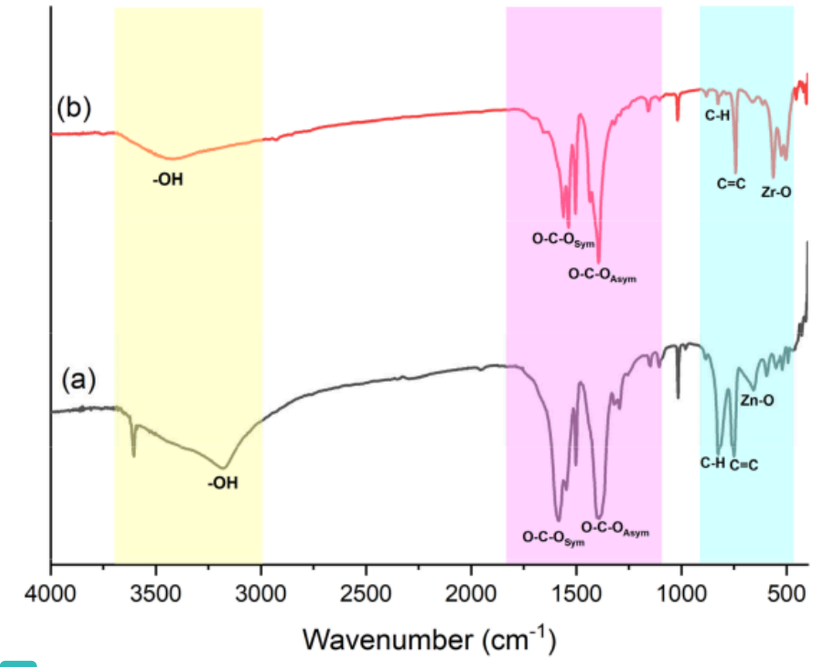

Fig 2. FTIR spectra of (a) Zn-MOF and (b) Zr-MOF

Table 1. Wavenumbers of Zn-MOF and Zr-MOF

Material	Wavenumber (cm^{-1})						
	ν O-H	ν –OCO-sym	ν –OCO-asym	ν C-H	ν C=C	ν Zn-O	ν Zr-O
Zn-MOF (this study)	3666-3036	1587	1392	827	748	651	
Zn-MOF [22]	3472	1585	1392	-	752	652	
Zn-MOF [23]	3500	1599	1387	-	-	530	
Zr-MOF (this study)	3658-3174	1562	1390	823	742		563
Zr-MOF [19]	3343	1572	1386	856	-		662
Zr-MOF [20]	3500	1597	1406	808	746		500

3.2.2 XRD analysis

The diffraction patterns of Zn-MOF and Zr-MOF are shown in Figure 3. The characteristic peaks of Zn-MOF in Figure 3(a) are observed at 2θ 6.8°, 9.6°, 13.72°, 15.44°, and 20.6°. These diffraction patterns for Zn-MOF are consistent with the findings of Dahlan *et al.* [17], who reported characteristic peaks and crystal planes of Zn-MOF at 6.8° (200), 9.6° (220), 13.8° (400), and 19.8° (440). Similar results were also reported by Burgaz et al.[24], showing characteristic peaks and crystal planes of Zn-MOF at 6.8° (200), 9.6° (220), 13.7° (400), and 15.3° (420). This study's 6.8° peak is higher than the 9.6° peak due to regular crystal morphology. Additionally, Figure 3(a) indicates that the 9.6° peak is split, suggesting distortion and a trigonal symmetry in the Zn-MOF structure [24–25].

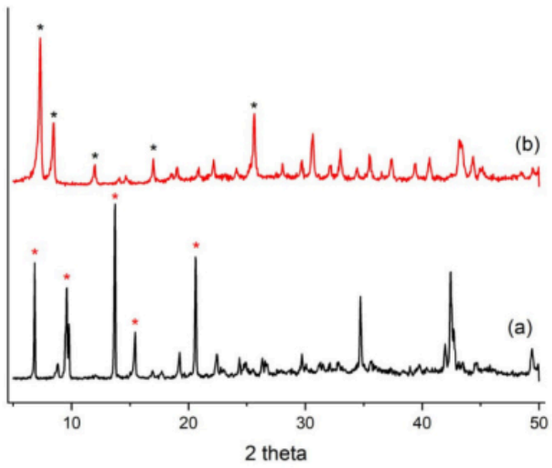

Fig 3. Diffraction Patterns: (a) Zn-MOF (b) Zr-MOF

The characteristic peaks of Zr-MOF in Figure 3(b) are shown at 2θ 7.32°, 8.48°, 11.9°, 14.0°, 14.6°, and 17.0°. The diffraction pattern of Zr-MOF corresponds to the findings of Lin *et al.* [21], who reported characteristic peaks and crystal planes of Zr-MOF at 7.3° (111), 8.5° (200), 14.8° (222), and 17.1° (400). Similar results were also reported by Hu *et al.* [15], who found characteristic peaks and crystal planes of Zr-MOF at 7.15° (111), 8.35° (200), 11.8° (220), 14.6° (222), and 17.1° (400). These results strengthen the successful synthesis of Zn-MOF and Zr-MOF in this study.

3.2.3 SEM analysis

The morphology of Zn-MOF and Zr-MOF are shown in Figure 4. Based on SEM analysis, Zn-MOF has a cubic surface structure, while Zr-MOF has a round or oval surface structure that aggregates together. These results are consistent with the study by AbouAitah *et al.* [12], which showed that Zr-MOF has irregularly shaped aggregated particles. These findings also align with the research by Burgaz *et al.* [24], who reported that Zn-MOF has a cubic surface structure. According to SEM analysis, the surface diameter of Zn-MOF is 248-391 nm, while the diameter of Zr-MOF is 26-42 nm. These results indicate successful synthesis of Zn-MOF and Zr-MOF.

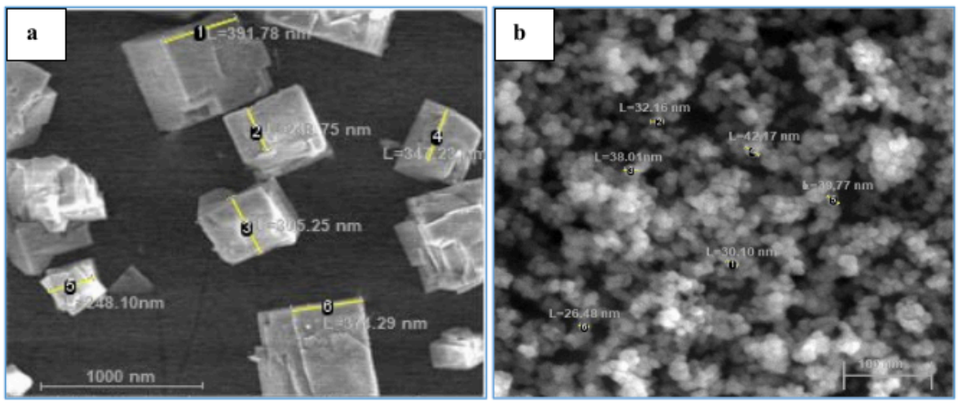

Fig 4. SEM Image (a) Zn-MOF (b) Zr-MOF

3.2.4 Antibacterial Test

The antibacterial efficacy of Zn-MOF and Zr-MOF were assessed by comparing their antibacterial activity results with the antibiotic amoxicillin. This study tested the antibacterial activity against *Escherichia coli* and *Staphylococcus aureus*, as they are commonly found bacteria causing infectious diseases and are resistant to some antibiotics or multidrug resistance [4–6]. The antibacterial activity results for Zn-MOF, Zr-MOF, and amoxicillin against *Escherichia coli* and *Staphylococcus aureus* are shown in Figure 5, with bacterial inhibition zones indicated in Table 2. Figure 5 demonstrates that Zn-MOF, Zr-MOF, and amoxicillin are sensitive to *Escherichia coli* and *Staphylococcus aureus* bacteria. MOF has sensitivity towards *Escherichia coli* and *Staphylococcus aureus* because MOF is capable of oxidizing and depolarizing the outer cell membrane of bacteria, and the central metal in MOF can damage bacterial proteins [11–26].

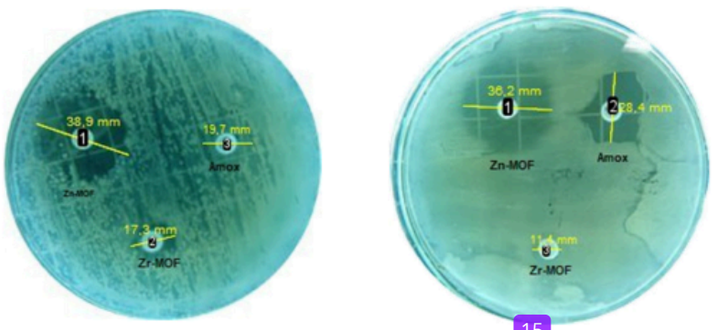

Fig 5. Sensitivity test results of Zn-MOF, Zr-MOF, and amoxicillin against *Escherichia coli* and Staphylococcus aureus.

Table 2. Comparison of inhibition zones of active substances against *Escherichia coli* and Staphylococcus aureus

Material	Concentration (mg/mL)	Bacterial zone inhibition (mm)		Reference
		Escherichia coli	Staphylococcus aureus	
APE	10	11±1	20±1	[27]
BAE	10	15±0.5	14±1	[27]
Zn-MOF	2	8.6±1.41	17±0.82	[11]
Amoxilin	25	28.4±1	19.7±1	this study
Zn-MOF	2	36.2±1	38.9±1	this study
Zr-MOF	2	11.4±1	17.3±1	this study

Table 2 shows that Zn-MOF has the largest inhibition zone, thus is recommended the development of Zn-MOF as an antibacterial material. Table 2 also indicates that the average inhibition zone of the active substance against *Escherichia coli* bacteria is lower than Staphylococcus aureus. *Escherichia coli* bacteria are more resistant to active substances because they are gram-negative bacteria with an outer membrane consisting of lipopolysaccharides that can protect against antibiotics and other active substances. MOF exhibit better antibacterial activity when compared to active substances from plants, such as *Andrographis paniculata extract* (APE) and *Berberis aristata extract* (BAE). This demonstrates the potential for MOF development as an antibacterial material. Table 2 also shows that MOF has large inhibition zone despite being used at a lower dosage concentration. This is consistent with the research by Akbarzade *et al.* [11], which reported that MOF has longer persistence than antibiotics, resulting in higher antibacterial efficiency even with lower doses.

In this study, Zn-MOF has a higher inhibitory zone against *Escherichia coli* and *Staphylococcus aureus* bacteria than Zr-MOF and amoxicillin. This result is driven by Zr-MOF has higher crystallinity than Zn-MOF, resulting in easier detachment of Zn-O bonds than Zr-O. The release of Zn metal in Zn-MOF leads to bacterial protein damage [26]. These findings also indicate that Zn-MOF can address bacterial resistance issues.

4 Summary

The results of analysis using ATR-FTIR showed that the Zn-MOF functional groups appear at wavelengths 3666-3036 cm^{-1} (νO-H), 1587cm^{-1} (ν–OCO-sym), 1392cm^{-1} (ν–OCO-asym), 837cm^{-1} (νC-H), 748cm^{-1} (νC=C) and 651cm^{-1} (νZn-O) while the Zr-MOF functional group appears at a wavelength of 3658-3174 cm^{-1} (νO-H), 1562cm^{-1} (ν–OCO-sym), 1390cm^{-1} (ν–OCO-asym), 823cm^{-1} (νC-H), 742cm^{-1} (νC=C) and 563cm^{-1} (νZr-O). The results of XRD analysis show that the characteristic peak of Zn-MOF is at 2θ 6.8°; 9.6°; 13.72°; 15.44°; 20.6° while the distinctive peak of Zr-MOF is shown at 2θ 7.32°; 8.48°; 11.9°; 14.0°; 14.6°; and 17.0°. Meanwhile, SEM results show that Zn-MOF has a cubic surface structure while Zr-MOF has aggregated particles with an irregular round shape. The results of the antibacterial test for *Staphylococcus aureus* showed that Zn-MOF (38.9 ± 1 mm) had the largest zone of inhibition, equivalent to the results of the antibacterial test for *Escherichia coli* showing that Zn-MOF (36,2±1 mm) has the largest zone of inhibition. The structural and morphological differences between the two MOFs, as evidenced by XRD and SEM analysis, significantly influence their physical and chemical properties. As a result, Zn-MOF exhibits stronger antibacterial activity than Zr-MOF, expectedly due to its crystallinity and release of Zn metal in Zn-MOF leads to bacterial protein damage.

The author express a gratitude to the Directorate General of Higher Education of the Ministry of Education and Culture of the Republic of Indonesia (DRTPM) for providing research funding through the grant "Penelitian Kerjasama Dalam Negeri" (PKDN), as well as to the Bhakti Wiyata Foundation, IIK Bhakti Wiyata, and Airlangga University for supporting the implementation of this research.

References

1. J. F. Fisher & S. Mobashery, Constructing and deconstructing the bacterial cell wall. *Protein science*, **29** (2020) 629–646.
2. M. A. Abushaheen, A. J. Fatani, M. Alosaimi, W. Mansy, M. George, S. Acharya, S. Rathod, D. D. Divakar, C. Jhugroo, & S. Vellappally, Antimicrobial resistance, mechanisms and its clinical significance. *Disease-a-Month*, **66** (2020) 100971.
3. Y. Li, P. Xiao, Y. Wang, & Y. Hao, Mechanisms and control measures of mature biofilm resistance to antimicrobial agents in the clinical context. *ACS omega*, **5** (2020) 22684–22690.
4. E. Bodendoerfer, M. Marchesi, F. Imkamp, P. Courvalin, E. C. Böttger, & S. Mancini, Co-occurrence of aminoglycoside and β-lactam resistance mechanisms in aminoglycoside-non-susceptible Escherichia coli isolated in the Zurich area, Switzerland. *International journal of antimicrobial agents*, **56** (2020) 106019.
5. B. Mlynarczyk-Bonikowska, C. Kowalewski, A. Krolak-Ulinska, & W. Marusza, Molecular mechanisms of drug resistance in Staphylococcus aureus. *International journal of molecular sciences*, **23** (2022) 8088.

6. P. Nikolic & P. Mudgil, The cell wall, cell membrane and virulence factors of Staphylococcus aureus and their role in antibiotic resistance. *Microorganisms*, **11** (2023) 259.
7. L. Poirel, J.-Y. Madec, A. Lupo, A.-K. Schink, N. Kieffer, P. Nordmann, & S. Schwarz, Antimicrobial Resistance in *Escherichia coli*. *Microbiology Spectrum*, **6** (2018). https://doi.org/10.1128/microbiolspec.ARBA-0026-2017.
8. A. Pantosti, A. Sanchini, & M. Monaco, Mechanisms of Antibiotic Resistance in *Staphylococcus Aureus*. *Future Microbiology*, **2** (2007) 323–334. https://doi.org/10.2217/17460913.2.3.323.
9. E. H. Haindongo, D. Ndakolo, M. Hedimbi, O. Vainio, A. Hakanen, & J. Vuopio, Antimicrobial resistance prevalence of Escherichia coli and Staphylococcus aureus amongst bacteremic patients in Africa: a systematic review. *Journal of Global Antimicrobial Resistance*, **32** (2023) 35–43. https://doi.org/10.1016/j.jgar.2022.11.016.
10. Y. Liu, L. Zhou, Y. Dong, R. Wang, Y. Pan, S. Zhuang, D. Liu, & J. Liu, Recent developments on MOF-based platforms for antibacterial therapy. *RSC Medicinal Chemistry*, **12** (2021) 915–928. https://doi.org/10.1039/D0MD00416B.
11. F. Akbarzadeh, M. Motaghi, N. P. S. Chauhan, & G. Sargazi, A novel synthesis of new antibacterial nanostructures based on Zn-MOF compound: design, characterization and a high performance application. *Heliyon*, **6** (2020).
12. K. AbouAitah, I. M. Higazy, A. Swiderska-Sroda, R. M. Abdelhameed, S. Gierlotka, T. A. Mohamed, U. Szałaj, & W. Lojkowski, Anti-inflammatory and antioxidant effects of nanoformulations composed of metal-organic frameworks delivering rutin and/or piperine natural agents. *Drug Delivery*, **28** (2021) 1478–1495.
13. Q. Gao, Q. Bai, C. Zheng, N. Sun, J. Liu, W. Chen, F. Hu, & T. Lu, Application of metal–organic framework in diagnosis and treatment of diabetes. *Biomolecules*, **12** (2022) 1240.
14. Y. Hu, H. Yang, R. Wang, & M. Duan, Fabricating Ag@MOF-5 nanoplates by the template of MOF-5 and evaluating its antibacterial activity. *Colloids and Surfaces A: Physicochemical and Engineering Aspects*, **626** (2021) 127093. https://doi.org/10.1016/j.colsurfa.2021.127093.
15. L. L. Zulfa, A. R. P. Hidayat, W. P. Utomo, R. Subagyo, E. N. Kusumawati, Y. Kusumawati, D. Hartanto, W. Widyastuti, & R. Ediati, Facile synthesis of Ni-ZIF-8 with improved photodegradation performance for methylene blue. *Case Studies in Chemical and Environmental Engineering*, **10** (2024) 100828. https://doi.org/https://doi.org/10.1016/j.cscee.2024.100828.
16. S. Elmehrath, K. Ahsan, N. Munawar, A. Alzamly, H. L. Nguyen, & Y. Greish, Antibacterial efficacy of copper-based metal–organic frameworks against Escherichia coli and Lactobacillus. *RSC advances*, **14** (2024) 15821–15831.
17. I. Dahlan, O. H. Keat, H. A. Aziz, & Y.-T. Hung, Synthesis and characterization of MOF-5 incorporated waste-derived siliceous materials for the removal of malachite green dye from aqueous solution. *Sustainable chemistry and pharmacy*, **31** (2023) 100954.
18. D. Villarroel-Rocha, M. C. Bernini, J. J. Arroyo-Gómez, J. Villarroel-Rocha, & K. Sapag, Synthesis of MOF-5 using terephthalic acid as a ligand obtained from polyethylene terephthalate (PET) waste and its test in CO2 adsorption. *Brazilian Journal of Chemical Engineering*, **39** (2022) 949–959.

19. F. Tian, R. Weng, X. Huang, G. Chen, & Z. Huang, Fabrication of Silver-Doped UiO-66-NH2 and Characterization of Antibacterial Materials. *Coatings*, **12** (2022) 1939.
20. M. Nasrabadi, M. A. Ghasemzadeh, & M. R. Z. Monfared, The preparation and characterization of UiO-66 metal–organic frameworks for the delivery of the drug ciprofloxacin and an evaluation of their antibacterial activities. *New Journal of Chemistry*, **43** (2019) 16033–16040.
21. X. Lin, W. Zeng, Y. Chen, T. Su, Q. Zhong, L. Gong, & Y. Liu, UiO-66-derived porous-carbon adsorbents: synthesis, characterization and tetracycline adsorption performance. *Carbon Letters*, **32** (2022) 875–884.
22. Y. Hu, H. Yang, R. Wang, & M. Duan, Fabricating Ag@ MOF-5 nanoplates by the template of MOF-5 and evaluating its antibacterial activity. *Colloids and Surfaces A: Physicochemical and Engineering Aspects*, **626** (2021) 127093.
23. G. Kumar & D. T. Masram, Sustainable synthesis of MOF-5@ GO nanocomposites for efficient removal of rhodamine B from water. *ACS omega*, **6** (2021) 9587–9599.
24. E. Burgaz, A. Erciyes, M. Andac, & O. Andac, Synthesis and characterization of nano-sized metal organic framework-5 (MOF-5) by using consecutive combination of ultrasound and microwave irradiation methods. *Inorganica Chimica Acta*, **485** (2019) 118–124.
25. M. Arjmandi, A. Altaee, A. Arjmandi, M. P. Chenar, M. Peyravi, & M. Jahanshahi, A facile and efficient approach to increase the magnetic property of MOF-5. *Solid State Sciences*, **106** (2020) 106292.
26. Y. Liu, L. Zhou, Y. Dong, R. Wang, Y. Pan, S. Zhuang, D. Liu, & J. Liu, Recent developments on MOF-based platforms for antibacterial therapy. *RSC Medicinal Chemistry*, **12** (2021) 915–928.
27. S. Abass, S. Zahiruddin, A. Ali, M. Irfan, B. Jan, Q. M. R. Haq, S. A. Husain, & S. Ahmad, Development of synergy-based combination of methanolic extract of Andrographis paniculata and Berberis aristata against E. coli and S. aureus. *Current Microbiology*, **79** (2022) 223.

Antibacterial Efficacy of Zinc and Zirconium Based Metal Organic Frameworks against Escherichia coli and Staphylococcus aureus

ORIGINALITY REPORT

17%	12%	9%	4%
SIMILARITY INDEX	INTERNET SOURCES	PUBLICATIONS	STUDENT PAPERS

PRIMARY SOURCES

1	journal.uin-alauddin.ac.id Internet Source	3%
2	iptek.its.ac.id Internet Source	1%
3	Ratna Ediati, Irmina Kris Murwani, Aldi Gunawan. "Synthesis and catalytic activity of mesoporous Al-MCM-41/UiO-66 for esterification of oleic acid", AIP Publishing, 2018 Publication	1%
4	Prachi Prachi, Asghar Ali, Mohammad Abid, Mohan Kamthan, Chhaya Ravi Kant. "Synergistic interaction of copper MOF and ciprofloxacin for enhanced antibacterial activity: A novel approach in biomedical materials and drug design strategy", Journal of Materials Research, 2025 Publication	1%
5	www.iau.edu.sa Internet Source	1%
6	worldwidescience.org Internet Source	1%
7	www.nveo.org Internet Source	1%
8	Rui Li, Tongtong Chen, Xiangliang Pan. "Metal–Organic-Framework-Based Materials	1%

for Antimicrobial Applications", ACS Nano, 2021
Publication

9	ethesis.nitrkl.ac.in Internet Source	1 %
10	Gyanendra Kumar, Navin Kumar Mogha, Dhanraj T. Masram. " Zr-Based Metal–Organic Framework/Reduced Graphene Oxide Composites for Catalytic Synthesis of 2,3-Dihydroquinazolin-4(1)-one Derivatives ", ACS Applied Nano Materials, 2021 Publication	<1 %
11	Michael Zuarez-Chamba, Saravanan Rajendran, Miguel Herrera-Robledo, A.K. Priya, Carlos Navas-Cárdenas. "Bi-based photocatalysts for bacterial inactivation in water: Inactivation mechanisms, challenges, and strategies to improve the photocatalytic activity", Environmental Research, 2022 Publication	<1 %
12	pubs.rsc.org Internet Source	<1 %
13	scholar.unair.ac.id Internet Source	<1 %
14	Submitted to Queen Mary and Westfield College Student Paper	<1 %
15	Sanober Gul, Hassanien Gomaa, Maryam Batool, De-Ming Kong, Li-Na Zhu. "A comprehensive review on advanced zirconium-based metal-organic frameworks: Rational design, critical properties, and versatile adsorptive applications in wastewater remediation", Journal of Environmental Chemical Engineering, 2026 Publication	<1 %

16	Taher Shahryari, Fateme Vahidipour, Narendra Pal Singh Chauhan, Ghasem Sargazi. " Synthesis of a novel / nanofibrous composite as bioorganic material: Design, systematic study and an efficient arsenic removal ", Polymer Engineering & Science, 2020 Publication	<1 %
17	Anatoli Davydov. "Molecular Spectroscopy of Oxide Catalyst Surfaces", Wiley, 2003 Publication	<1 %
18	Submitted to University of Sheffield Student Paper	<1 %
19	opus.bath.ac.uk Internet Source	<1 %
20	scholar.uoc.ac.in Internet Source	<1 %
21	acikerisim.omu.edu.tr Internet Source	<1 %
22	etheses.durham.ac.uk Internet Source	<1 %
23	link.springer.com Internet Source	<1 %
24	sjpas.univsul.edu.iq Internet Source	<1 %
25	www.science.gov Internet Source	<1 %
26	Shibyendu Nikhar, Mitun Chakraborty, Pawan Kumar. "Relative capability analysis on carboxylate and imidazole based MOFs for PVP and PSS photo catalytic degradation in water", Inorganic Chemistry Communications, 2023 Publication	<1 %

27	agribalkan.congress.gen.tr Internet Source	<1 %
28	asianpubs.org Internet Source	<1 %
29	dokumen.pub Internet Source	<1 %
30	pubblicazioni.unicam.it Internet Source	<1 %
31	ugspace.ug.edu.gh Internet Source	<1 %
32	www.sciencegate.app Internet Source	<1 %
33	Submitted to Brigham Young University Student Paper	<1 %

Exclude quotes	On	Exclude matches	Off
Exclude bibliography	On		

Antibacterial Efficacy of Zinc and Zirconium Based Metal Organic Frameworks against Escherichia coli and Staphylococcus aureus

GRADEMARK REPORT

FINAL GRADE

/100

GENERAL COMMENTS

PAGE 1

PAGE 2

PAGE 3

PAGE 4

PAGE 5

PAGE 6

PAGE 7

PAGE 8

PAGE 9

PAGE 10